energies

MDPI

Article

Verification and Validation of CFD Modeling for Low-Flow-Coefficient Centrifugal Compressor Stages

Vycheslav Ivanov [1], Yuri Kozhukhov [2,*], Aleksei Danilishin [3], Aleksey Yablokov [3] and Michail Sokolov [3]

[1] National Technological Initiative Center of Excellence in New Manufacturing Technologies, Peter the Great St. Petersburg Polytechnic University, 195251 Saint-Petersburg, Russia; slavanw@bk.ru
[2] Center for Industrial, Resource and Infrastructure Expertise and Management, Peter the Great St. Petersburg Polytechnic University, 195251 Saint-Petersburg, Russia
[3] High School of Energy Engineering, Peter the Great St. Petersburg Polytechnic University, 195251 Saint-Petersburg, Russia; danilishin_am@mail.ru (A.D.); yablokovaleksey@mail.ru (A.Y.); smi1994spb@gmail.com (M.S.)
* Correspondence: kozhukhov_yv@mail.ru; Tel.: +7-921-567-8491

Abstract: In this paper, the numerical model of a centrifugal compressor low-flow stage is verified. The gaps and labyrinth seals were simulated in the numerical model. The task was to determine the optimal settings for high-quality modeling of the low-flow stages. The intergrid interface application issues, turbulence and roughness models are considered. The obtained numerical model settings are used to validate seven model stages for the range of the optimal conditional flow coefficient with Φ_{opt} = 0.008–0.018 and the conditional Mach number M_u = 0.785–0.804. The simulation results are compared with the experimental data. The high pressure stage-7 (HPS-7) stage with Φ_{opt} = 0.010 and M_u = 0.60 at different inlet pressure of 4, 10 and 40 atm is considered separately. Acceptable validation results are obtained with the recommended numerical model settings; the modeling uncertainty for the polytropic pressure coefficient δη*pol < 4% for the efficiency coefficient δη*pol exceeds the limit of 4% only in the two most low-flow stages, U and V.

Keywords: centrifugal compressor; CFD; verification; validation; low flow; digital twin

Citation: Ivanov, V.; Kozhukhov, Y.; Danilishin, A.; Yablokov, A.; Sokolov, M. Verification and Validation of CFD Modeling for Low-Flow-Coefficient Centrifugal Compressor Stages. *Energies* **2022**, *15*, 181. https://doi.org/10.3390/en15010181

Academic Editors: Dmitri Eskin and Christopher Micallef

Received: 8 November 2021
Accepted: 24 December 2021
Published: 28 December 2021

1. Introduction

Improving the efficiency of centrifugal compressor low-flow stages is hindered due to the small relative width of the flow part channels [1]. In such stages, the following features play a significant role: closing of the boundary layers in the meridional section, increase of friction loss and leak, strong secondary flows, and a more intense low-energy zone on the back of the impeller blades. Standard design methods for industrial compressors in low-flow stages have increased and unacceptable uncertainty; thus, the results of viscous flow calculations are used for the design. Initially, the quasi-three-dimensional inviscid flow calculations with boundary layer estimation and three-dimensional viscous flow calculations on very coarse meshes are used. Currently, in centrifugal compressor design and manufacturing practice computational fluid dynamics methods (CFD) are used to calculate and analyze a viscous three-dimensional turbulent flow in the flow part. CFD methods are used for fine-tuning existing designs of compressors and power engineering equipment in order to increase efficiency [2–4]. For this purpose, multivariate optimization can be used to obtain a Pareto set of optimal solutions. In addition, the calculated loss flow part elements coefficients can be used in one-dimensional methods of designing centrifugal compressors. CAD design models of centrifugal compressor stages can be used as virtual models for working in various technological processes or as independent units for checking the quality of the project instead of experimental work. In this way, changes can be made to the project before it is made. The numerical model must be correctly configured with a known modeling uncertainty level. Numerical methods must be verified and validated

before being applied [5]. The largest number of works are concentrated on medium- and high-flow stages with 3D impellers, while relatively few works are concentrated on the verification and validation of numerical calculations with experimental data in stages with low-flow coefficients [6–13]. The estimation of the modeling uncertainty for low-flow stages in the available literature is presented in Table 1. The table shows that most of the stages are close to the upper bound of the low-flow stages, with $\Phi_{des} = 0.024 \ldots 0.028$. Three works [6,7,10] relate to stages with $\Phi_{des} < 0.02$. In the first work, only the impeller is calculated, and in the second there is no specific data on the uncertainty in the stage, and the uncertainty value for the entire compressor is recalculated using a one-dimensional technique. Large uncertainty in [8] is due to unaccounted gaps and seals. The full stages are presented in four works [10–13]. In [10], an increased uncertainty of more than 10% for the pressure coefficient is obtained, along with up to 3% for the rest. As the low-flow stages are typically the end stages of multi-stage compressors, these stages have narrow flow sections and increased loss levels, and designers try to avoid using them; however, in some cases it is not possible to proceed without them. For low-flow stages, it is necessary to study the full design model, taking into account leaks in gaps and labyrinth seals.

Table 1. The results of the research in the available literature.

Source	CFD Model Description	Φ_{des}	M_u	Relative Uncertainty, δ
Voronova et al., 1997 [6]	STAR-CD; Grid: 80,000; k-ε; 2D impeller only;	0.016	0.60	for pressure ratio: π_2 = 1.5–2%
Biba et al., 2002 [7]	CFX-Tascflow; Grid: 150,000; without gaps and seals;	0.0275 0.0146 0.0117	-	2.5% based on stage-by-stage calculation overall compressor performance prediction
Tanaka et al., 2008 [9]	CFX-11.0; Grid: 400,000; k-ε; without gaps and seals	0.021	0.85	no data
Lettieri et al., 2014 [10]	Ansys CFD; Full stage SST; Grid: 11,000,000	0.003	0.75	η^*_{pol} = 1–13% ψ = 12%
Kabalyk et al., 2016 [8]	Ansys CFX 16.2; Grid:690 000; SST; without gaps and seals	0.024	0.70	π = 1–4%; η_s = 11%; ψ_i = 8–14%
Yablokov et al., 2018 [12]	Ansys CFX 14.0; Grid:4 500,000 SST; Full stage	0.028	0.60	η^*_{pol} = 2–3%; ψ_i = 2–3%; ψ_t = 2–3%
Hazby et al., 2019 [11]	Ansys CFX 17.1; Grid:4 000,000 SST; Full stage	0.0265	0.90	η_{pol} = 3%; ψ_i = 3%; Estimation from the figures

In the previous work [14] verification and validation were performed for complete numerical models of two medium-flow stages. An acceptable modeling uncertainty is obtained with no more than 2% on the design mode with $\Phi_{des} = 0.064$ and $\Phi_{des} = 0.055$. Regarding low-flow stages, Ref. [15] the design model of only the impeller is considered. The results of the non-viscous and viscous calculation for the characteristic of the theoretical head ψ_t are compared in the paper. It is confirmed that when designing low-flow stages it is necessary to use only viscous methods, unlike medium and high-flow stages. In [12] a complete stage with $\Phi_{des} = 0.028$ is considered, however, this stage has sufficiently wide channels that the features of low-divergent stages are little manifested.

In this paper, the feasibility of considering modeling in stages with $0.008 < \Phi_{opt} < 0.020$ is investigated and the modeling uncertainty values are determined for some low-flow-coefficient stages. Modeling uncertainty levels can be used in design optimization as well as numerical methods improvement [16].

Therefore, the aim of this work is to determine which optimal settings for the numerical model provide acceptable modeling uncertainty in comparison with the experimental data.

The level of modeling uncertainty for the stages with low-flow rate coefficient is estimated. The novelty of this work lies in the data generalization on the modeling uncertainty in low-flow stages with a range of flow coefficient 0.008 < Φopt < 0.020 and the recommendations issuance for qualitative modeling.

2. Materials and Methods

The objects of research were the low-flow model stages of the XX3B base with impellers of the Q, R, S, T, U, and V series; the license for these stages of the Dresser and Clark company was acquired by the USSR in the early 1970s. The intermediate stage consists of the following elements: a 2D impeller (imp.), a vaneless diffuser (VLD), a return channel (RC), a deswirl vane, and gaps and labyrinth seals (l. s.) at the hub and shroud disks. The gaps and labyrinth seals were developed based on the experience of the Ultra-High Pressure group [17], as the original drawings of these elements were not available. Three VLD's were used for the stages, one for the Q and R series, the second for the S and T series, and the third for the U and V series. The return channel was the same for all stages and each second blade had an extension in the form of a radial continuation. The characterizations of the main stages used are shown in Table 2. Overline refers to a dimensionless form obtained by dividing by impeller radius R_2. The dimensions can be found in Figure 1a. The analysis was carried out on the basis of available experimental data on seven stage models for the range of optimal conditional flow coefficient with Φ_{opt} = 0.008–0.018. For stages Q, the Mach number at the impeller outlet was Mu = u_2/a = 0.785 (here u_2 is peripheral speed, ais sound speed), and for the rest is M_u = 0.802. Data for the experimental error did not exist; therefore, it was taken as the standard relative experimental relative uncertainty δ = 4% in accordance with [18].

Table 2. Main used stages characterizations of model stages of base XX3B.

№ Stage	Flow Coefficient Φ_{opt}	Entrance Relative Radius of the Impeller Blade $\bar{R}_1$	Relative Radius of Impeller Inlet $\bar{R}_0$	Relative Radius of Impeller Hub $\bar{R}_h$	Relative Blade Height $\bar{b}_1$=$\bar{b}_2$	Number of Impeller Blades z, Pcs
1-Q482	0.018	0.5063	0.434	0.355	0.0263	15
2-Q508	0.015	0.4822	0.414	0.338	0.0250	15
3-R508	0.013	0.4822	0.414	0.338	0.0217	15
4-S508	0.012	0.4822	0.414	0.338	0.0189	15
5-T508	0.011	0.4822	0.414	0.338	0.0164	15
6-U508	0.009	0.4822	0.414	0.338	0.0143	15
7-V508	0.008	0.4822	0.414	0.338	0.0124	15

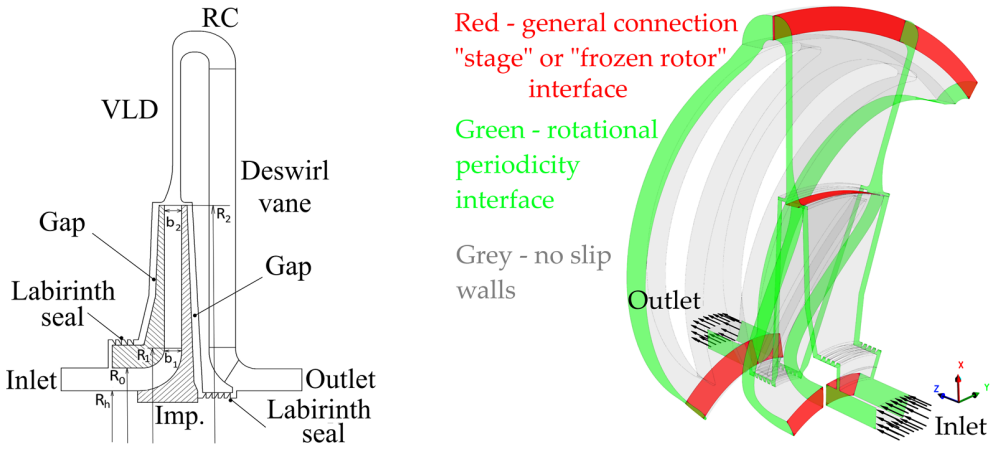

Figure 1. (**a**) Sketch of the flow part meridional view; (**b**) numerical model of the stage.

The study is divided into two stages: verification and validation. At the verification stage for the Q482 stage, the following tasks were investigated: research on the grid independence solution, research on the applied turbulence models, research on intergrid interfaces and research on the influence of roughness. As a result, the optimal settings of the numerical model were determined. At the validation stage, the refined numerical model was used to estimate the uncertainty of numerical modeling by comparing it with experimental data.

The stage diagram and numerical model are shown in Figure 1. The design model consists of seven design domains: inlet, impeller, VLD, RC with deswirl vane, left gap with l. s., right gap with l. s., outlet. The impeller is presented as a rotating domain and the rest are stationary, in which the option of rotating impeller walls in gaps is used. In total, seven numerical models of the stages, presented in Table 2, were constructed. The size of the main computational grids was about ~4 million elements. The working medium was an ideal gas. The total inlet pressure was 98,000 Pa and the total temperature was 288 K, and the mass flow rate was set at the outlet. Medium inlet turbulence level was set. The dimensionless parietal coordinate for all aims was no more than $y^+ < 2$. A stationary solution of the RANS equations was made. The Ansys CFX 18.0 solver was used. Convergence was achieved by unbalances and invariance of energy characterizations. The level of residuals in the main balance equations was less than 10^{-4}.

When studying the grid independence of the Q482 stage numerical model, additional computational grids were constructed separately. In particular, eight grids of impellers were studied with different expansion ratios r. A double calculation was performed with a twofold increase in the size of the main grid to ~8 mln. Three turbulence models, shear stress transport (SST), k-ω, and baseline k-ω (BSL), were considered. The intergrid interface stage (passing parameters averaged for the circumferential coordinate at the boundaries of the connection computational grids with stage constant pressure option) and frozen rotor (passing without averaging) were considered. Interfaces were considered in three downstream locations: after the impeller, after the VLD, and after the RC with deswirl vane. The circumferential location of the domains was not considered. This was because the impeller domain and the VLD had the same sweep angle and the assumption of stage nonuniformity disappearance at the 1.2–1.4 D_2 from the impeller, according to the known data; the other low-flow stages in [15] show a similar result. Therefore, it was advisable to consider this for low-flow stages as well. Finally, the effect of equivalent sand walls roughness of 1, 5, 10 μm compared to hydraulically smooth walls was considered. The rough walls option was used.

Based on the verification calculation results, the k-ω model was used to validate the calculated characterizations. The stage interface was selected behind the impeller; in the rest, frozen rotor and hydraulically smooth walls were chosen.

Processing of the results was carried out according to the following dependencies.

Flow coefficient is:

$$\Phi = \frac{4\overline{m}}{\rho_0^* \pi D_2^2 u_2}, \quad (1)$$

where $\overline{m}$ is mass flow and ρ_0^* is inlet total density.

Internal head coefficient is

$$\psi_i = \frac{c_p \Delta T^*}{u_2^2} = \frac{\Delta i^*}{u_2^2}, \quad (2)$$

where c_p is heat capacity at constant pressure, ΔT^* is total temperature difference, and Δi^* is total enthalpy difference.

Theoretical head coefficient is

$$\psi_t = c_{u2}/u_2, \quad (3)$$

where c_u is circumferential velocity.

Polytropic head coefficient on total parameter is

$$\psi^*_{pol} = \left(\frac{n}{n-1} RT_0 \left(\pi^{\frac{n-1}{n}} - 1 \right) + \frac{c_i^2 - c_0^2}{2} \right) / u_2^2, \quad (4)$$

where n is polytropic exponent, R is the gas constant, and c is absolute velocity,

Polytropic efficiency on total parameter is found by

$$\eta^*_{pol} = \psi^*_{pol} / \psi_i. \quad (5)$$

Absolute deviation (by parameter P) is

$$\Delta = \left| P_{\text{calc}.i} - P_{\text{exp}.i} \right|. \quad (6)$$

3. Results

3.1. Verification Results

To study the grid independence of the solution, eight calculated grids of the impeller were constructed from elements number-N 0.6 to 6.5 million, with a change in the expansion ratio r from 1.5 to 1.05. The size of the first grid element is y = 0.001 mm, which corresponds to the value y+ < 2, falling into the region of a viscous sublayer. The comparison was made by the coefficients of theoretical and polytropic pressure. No significant differences were found in the calculation results, as illustrated in Figure 2. In addition, a double calculation with the calculated grid increased by two times did not show any difference in the results. Thus, grid independence of the solution is achieved. For all elements of the stage, the expansion coefficient was set to r = 1.3.

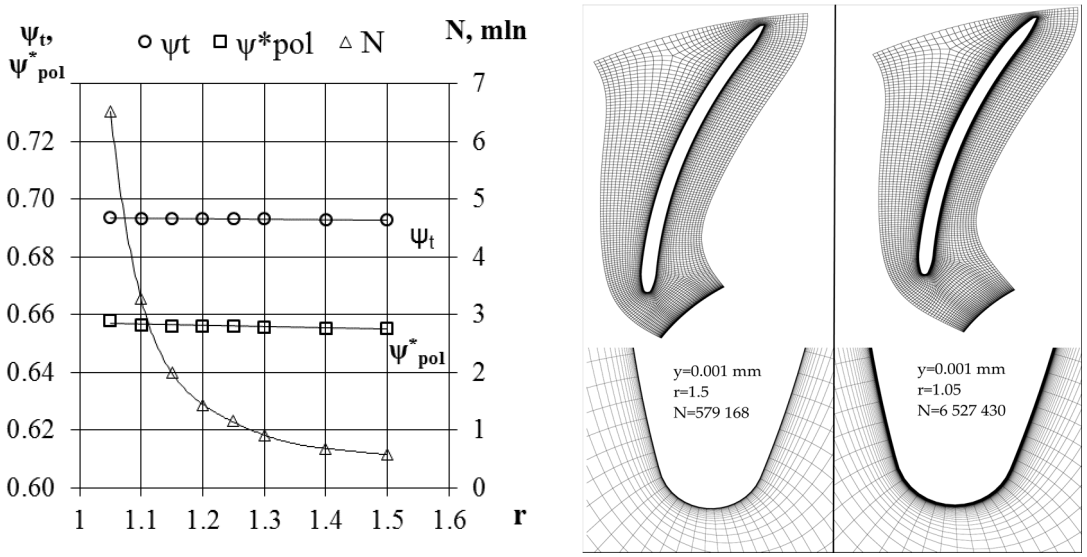

Figure 2. Impeller mesh independent study.

The first study was of the frozen rotor interface type stage. Comparison with the experimental data in Figure 3a shows a qualitative difference between the characterizations. Therefore, it is recommended to use the stage interface in low-flow as well as medium-flow stages with closed impellers. Next, the change in downstream interface location was considered; it is shown that this has little effect on the final results. Figure 3b shows that when the "frozen rotor" interface is replaced sequentially with the "Stage", the results change little. Here CFD(s) means that the «stage» is installed only after the impeller, CFD(ss) means behind the impeller and the vaneless diffuser, and CFD(sss) means in all inter-grid interfaces with different pitch angle and coordinate frame (rotating and

stationary). Therefore, it is advisable to use the stage interface only behind the impeller, and in other cases to use the frozen rotor. In addition, this reduces computational costs.

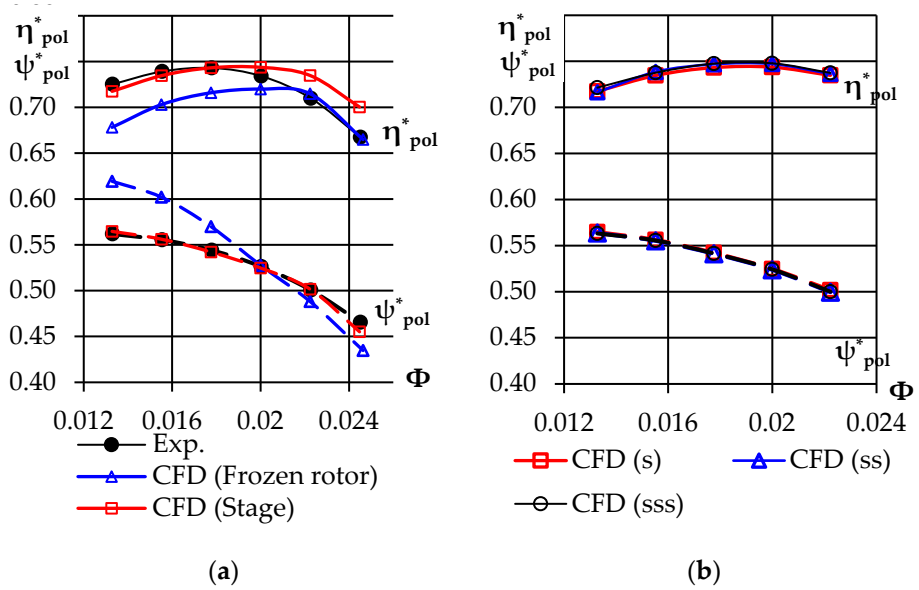

(**a**) (**b**)

Figure 3. Results of the intergrid interface study on the results of modeling the Q-482 model stage (**a**) interface type; (**b**) interface downstream location. s—stage interface after impeller only, ss—stage interface after impeller and vaneless diffuser, sss—stage at all intersectional interfaces.

Three turbulence models used for low-Reynolds computational grids ($y^+ < 2$) were considered. Results of the study can be observed on Figure 4. The highest accuracy was obtained using the k-ω model. Using the BSL model showed a result close to k-ω. When calculating with the SST model, a decrease of ψ^*_{pol} by ~2% relative to k-ω was obtained, with a difference of 0.5% for η^*_{pol}. For further calculations, the k-ω model was chosen as the basis.

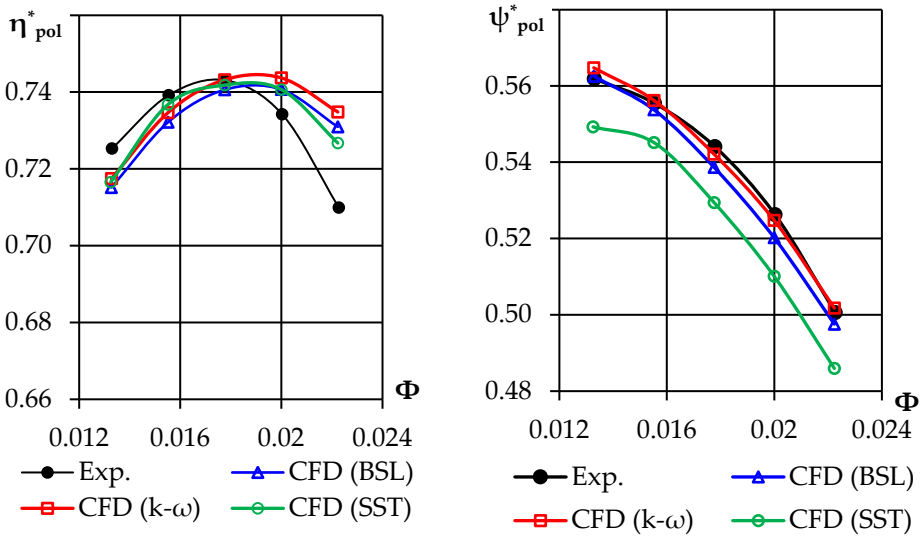

(**a**) (**b**)

Figure 4. Results of the study of the turbulence model influence on the results of modeling the Q-482 model stage: (**a**) Polytropic efficiency on total parameter; (**b**) Polytropic head coefficient on total parameter.

The influence of roughness on gas dynamic characterizations under increasing pressure is known [19]. The effect of roughness is especially significant in low-flow stages. In this study, a change in the equivalent sand roughness affected the characterizations when the value changed from 1 to 10 microns. The characteristics are shown in Figure 5. However, the closest to the experimental curve was shown to be hydraulically smooth walls. This is due to the fact that air tests are carried out at the inlet pressure.

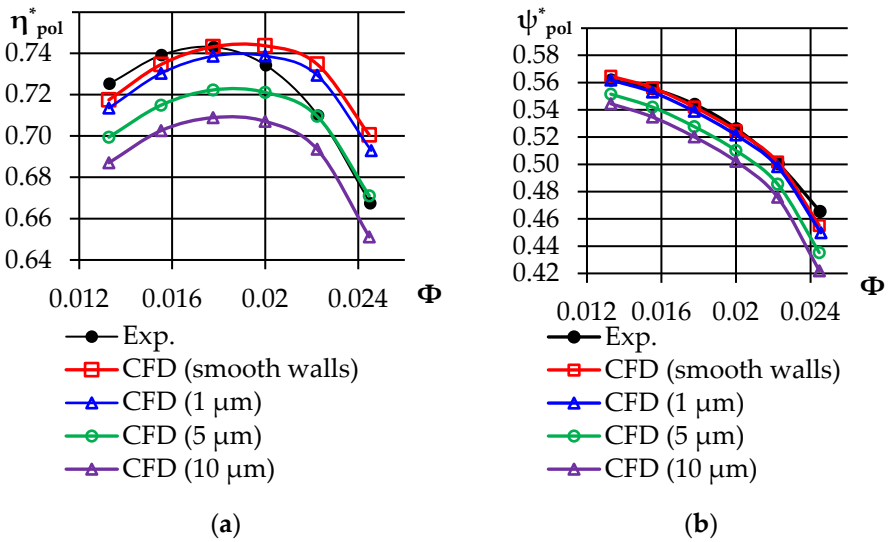

Figure 5. Results of the sand roughness influence study on the results of modeling the Q-482 model stage: (**a**) Polytropic efficiency on total parameter; (**b**) Polytropic head coefficient on total parameter.

Figure 6 shows the flowchart for setting boundary conditions and domain properties. Using the proposed settings of the numerical model allows for approaching the experimental curve more qualitatively and quantitatively. To validate the settings of the numerical model, their use for the other stages indicated in Table 2 is evaluated.

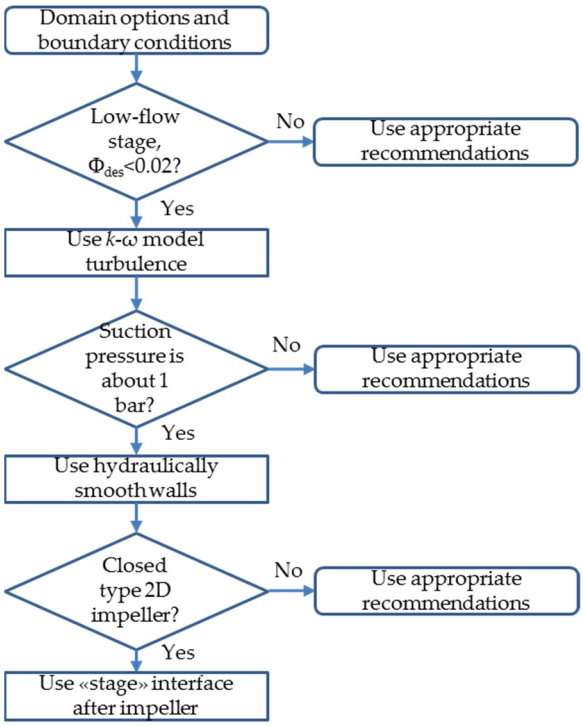

Figure 6. Recommendations flowchart for the low-flow stages with 2D closed type impeller.

3.2. Validation Results

The graphs of the characterizations in Figure 7 show that the simulation satisfac-torily repeats the characterization of the experimental curve forms. The characteriza-tions of the polytropic pressure are most qualitatively repeated with the total parame-ters. The maximum modelling uncertainty is observed in the maximum flow rate, which is also typical for medium-flow stages. With a decrease in the flow rate of a stage, the difference between the calculated and experimental efficiency increases. The level of uncertainty for the efficiency coefficient δη*pol exceeds the limit of 4% in the lowest-flow stages U and V. In general, the validation results can be considered ac-ceptable for the polytropic pressure coefficient δψ*pol < 4%.

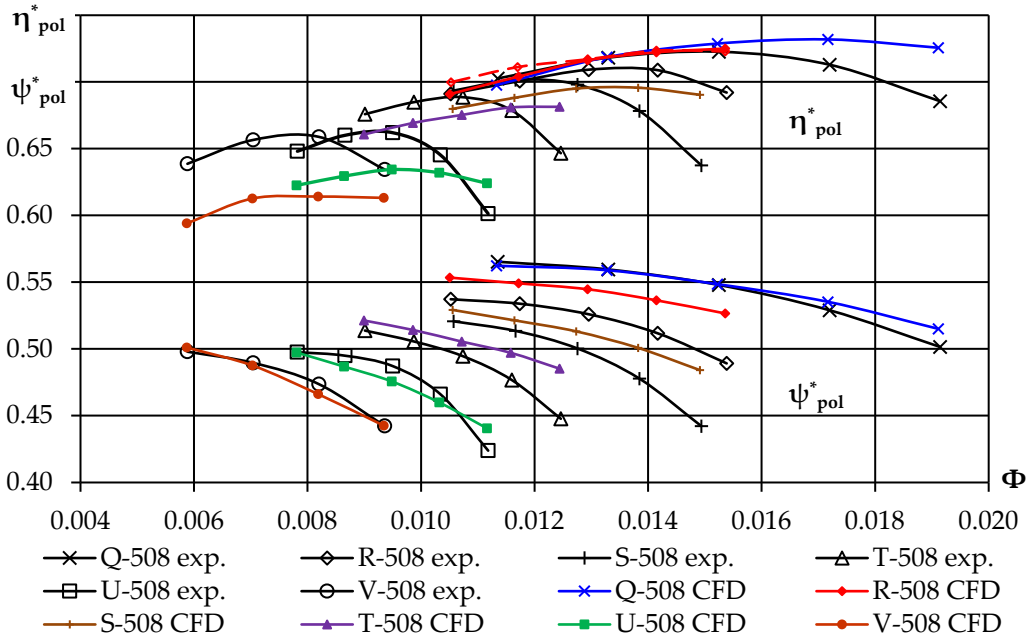

Figure 7. Comparison of experimental and calculated characterizations of the model stages.

In the optimal mode, the deviation range for the efficiency coefficient was $\Delta\eta^*_{pol}$ = 0.6 ... 4.4% absolutely, and for the polytropic pressure coefficient $\Delta\psi^*_{pol}$ = 0.001 ... 0.019 absolutely.

Due to the lack of data on the considered problems, the seals and gaps in all stages were the same, which could affect the final results. In addition, not enough is known about the thermal insulation of the housing and the test methods of the stages. Therefore, this issue will be studied separately with more verified data.

Figure 8 shows a section of the experimental test rig of the closed loop, LPI-SPbPU. The location of the model stage inside the main housing with the outlet gas flow provides an adiabatic problem statement when the steady-state mode is reached. The location of the measuring sections behind the impeller and the vaneless diffuser allows study of the characterizations of the model stage element by element. In this paper, a low-flow model HPS-7 stage with a calculated Φ_{des} = 0.008 is considered, tested at a Mach number of M_u = 0.60 [17].

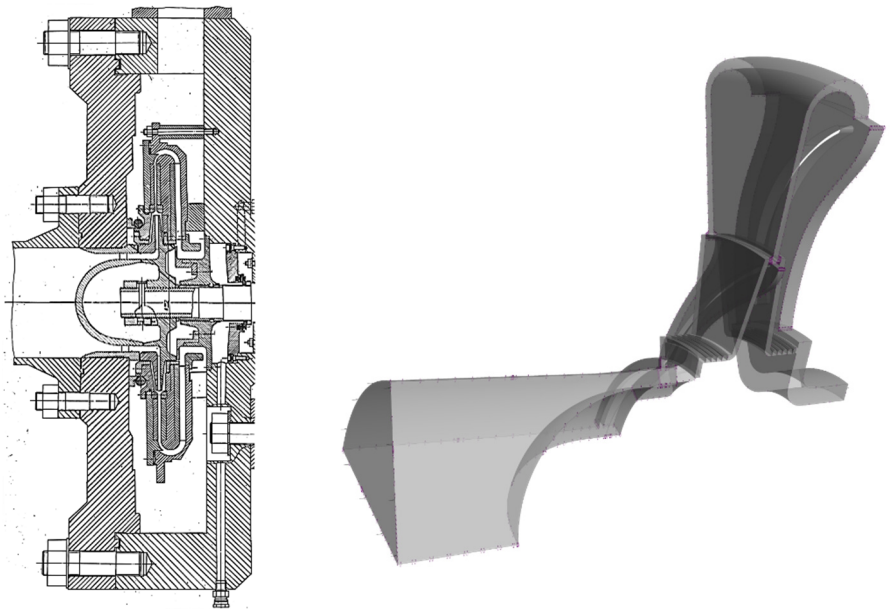

(**a**) (**b**)

Figure 8. (**a**) Experimental setup a closed loop and (**b**) numerical model of the HPS-7 stages.

The numerical model of the HPS-7 stage is based on the same principles as described above. Calculations were performed on fluid–nitrogen, with inlet pressures of 4, 10 and 40 atmospheres.

Figure 9 shows the characterizations of polytropic efficiency and the head coefficient on total parameters. In the optimal mode, the deviation range for the efficiency coefficient was $\Delta\eta^*_{pol} = 1.2 \ldots 3.2\%$ absolutely, while for the polytropic pressure coefficient it was $\Delta\psi^*_{pol} = 0.012 \ldots 0.022$ absolutely.

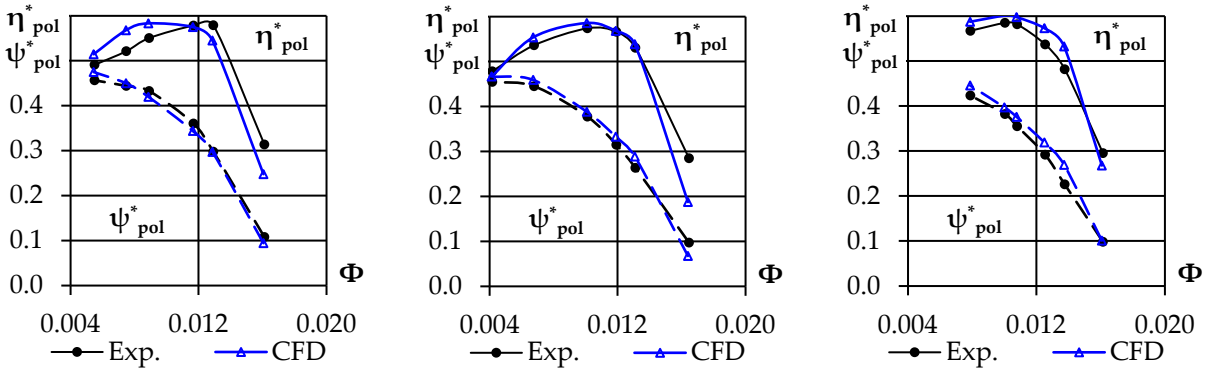

(**a**) (**b**) (**c**)

Figure 9. Comparison of experimental and calculated model stage characterizations with (**a**) 4 atm, (**b**) 10 atm, and (**c**) 40 atm.

The results of modeling the HPS-7 stage are in good agreement with the results of Q, R, S, T, U, and V. A more qualitative pattern of experimental curve repetition can be noted. When the inlet pressure increases from 4 to 40 atm, the uncertainty does not change very much.

4. Conclusions

The optimal settings of a low-flow stage numerical model are determined in this paper. As a result of the numerical model verification, it can be concluded that for low-flow stages

it is advisable to use the low-Reynolds turbulence model k-ω. The choice of k-ω is due to the fact that the boundary layer effects are more pronounced in low-flow stages, while SST shows good results when modeling medium-flow stages. The stage interface must be used to connect the grid models of a rotating impeller and a stationary vaneless diffuser without specifying the roughness of the walls, which should be left them hydraulically smooth if the inlet pressure is 1 atm. The uncertainty level for the polytropic pressure coefficient is acceptable for all stages in the optimal mode. The stage efficiency is underestimated due to an overestimation of the simulated internal pressure coefficient over the experimental values. This difference increases as the stage consumption decreases. In the high-flow mode, the low-flow stage characterization is similar to the medium-flow stage. Here, a computational model has been developed for the multivariate analysis of low-flow stages. The results of verification and validation were used to create mathematical models based on numerical databases [20]. Further work is should involve an increase in operating pressure and the issuance of recommendations on the use of wall roughness settings.

Author Contributions: Conceptualization, Y.K. and V.I.; Methodology, V.I.; Software, V.I., A.Y. and A.D.; Validation, V.I., Y.K., A.Y. and A.D.; Formal Analysis, Y.K., V.I., M.S. and A.Y.; Investigation, Y.K., V.I., A.Y. and A.D.; Writing—original draft preparation, V.I. and A.D.; Writing—review and editing, V.I. and M.S.; Supervision, Y.K. All authors have read and agreed to the published version of the manuscript.

Funding: This research was done by Peter the Great St. Petersburg Polytechnic University and supported under the strategic academic leadership program 'Priority 2030' of the Russian Federation (Agreement 075-15-2021-1333 dated 30 September 2021).

Acknowledgments: The calculations were performed using the supercomputer center SCC "Polytechnic", Peter the Great St. Petersburg Polytechnic University.

Conflicts of Interest: The authors declare no conflict of interest.

References

1. Seleznev, K.P.; Strizhak, L.Y. Thermogasdynamical basis for the high and ultra-high pressure compressor design. *Khimicheskoe I Neftegazov. Mashinostroenie* **1995**, *11*, 8–15.
2. Danilishin, A.M.; Kozhukhov, Y.V.; Kartashov, S.V.; Lebedev, A.A.; Malev, K.G.; Mironov, Y.R. Design optimization opportunity of the end stage output plenum chamber of the centrifugal compressor for gas pumping unit. *AIP Conf. Proc.* **2018**, *2007*, 030044. [CrossRef]
3. Han, L.; Li, F.; Li, N.; Zhou, H.; Jiang, L.; Wang, Z. The Development of High Efficiency Integrally Geared Driven Multistage Centrifugal Compressor. *Int. J. Fluid Mech. Therm. Sci.* **2020**, *6*, 53–60. [CrossRef]
4. Aytaç, Z.; Yücel, N. Development of a Design Methodology for a Centrifugal Compressor with the Utilization of CFD. *J. Polytech.* **2019**, *23*, 231–239. [CrossRef]
5. ASME. *Standard for Verification and Validation in Computational Fluid Dynamics and Heat Transfer—An American National Standard*; The American National Standard (ASME): New York, NY, USA, 2009; 100p.
6. Voronova, Y.A. *Chislennoe Issledovanie Techeniya Vyazkogo Gaza v Malorasxodnom Centrobezhnom Kolese Kanal'Nogo Tipa/*; Yu, A., Voronova, K.P., Seleznev, N.I., Sadovskij, L.Y., Strizhak, I.P., Suslina, V., Riss, E., Eds.; Etter.//E'nergeticheskie mashiny' i ustanovki. Trudy' SPbGTU. No. 465; Publishing House of SPbSTU: St. Petersburg, Russia, 1997; pp. 3–8.
7. Biba, Y.I.; Nye, D.A.; Liu, Z. Performance Evaluation and Fluid Flow Analysis in Low Flow Stages of Industrial Centrifugal Compressor. *Int. J. Rotating Mach.* **2002**, *8*, 309–317. [CrossRef]
8. Kabalyk, K.; Kryłłowicz, W. Numerical modeling of the performance of a centrifugal compressor impeller with low inlet flow coefficient. *Trans. IFFM* **2016**, *131*, 97–109.
9. Tanaka, M.; Kobayashi, H.; Nishida, H. Development of Wedge Type Impellers for Low Specific Speed Centrifugal Compressors. In Proceedings of the 2008 ASME International Mechanical Engineering Congress and Exposition, Boston, MA, USA, 31 October–6 November 2008. [CrossRef]
10. Lettieri, C.; Baltadjiev, N.; Casey, M.; Spakovszky, Z.S. Low-Flow-Coefficient Centrifugal Compressor Design for Supercritical CO_2. *J. Turbomach.* **2014**, *136*, 081008. [CrossRef]
11. Hazby, H.; Casey, M.; Brezina, L. Effect of Leakage Flows on the Performance of a Family of Inline Centrifugal Compressors. *J. Turbomach.* **2019**, *141*, 091006. [CrossRef]
12. Yablokov, A.; Yanin, I.; Danilishin, A.; Zuev, A. Ansys CFX numerical study of stages centrifugal compressor with low-flow rate coefficient. *MATEC Web Conf.* **2018**, *245*, 09002. [CrossRef]

13. Yablokov, A.; Yanin, I.; Sadovskyi, N.; Kozhukhov, Y.; Nguyen, M.H. Numerical characteristics of a centrifugal compressor with a low flow coefficient. *E3S Web Conf.* **2019**, *140*, 06010. [CrossRef]
14. Gileva, L.; Kartashov, S.; Zuev, A.; Ivanov, V. Verification of the CFD calculation for the centrifugal compressor medium flow model stages with the help of supercomputer. *MATEC Web Conf.* **2018**, *245*, 09011. [CrossRef]
15. Ivanov, V.M.; Kozhukhov, Y.V.; Danilishin, A.M. Calculation of the impellers head characteristics of the low-flow centrifugal compressor stages based on quasi-three-dimensional inviscid and viscous methods. *AIP Conf. Proc.* **2019**, *2141*, 030064. [CrossRef]
16. Neverov, V.V.; Kozhukhov, Y.V.; Yablokov, A.M.; Lebedev, A.A. The experience in application of methods of computational fluid dynamics in correction of the designed flow path of a two-stage compressor. *AIP Conf. Proc.* **2018**, *2007*, 030048. [CrossRef]
17. Strizhak, L.Y. Issledovanie Centrobezhny'x Kompressorov vy'sokogo i Sverxvy'sokogo Davleniya [E'lektronny'j Resurs]/L.Ya. Strizhak.—E'lektron Tekstovy'e dan. (1 Fajl: 796 Kb)//Trudy' Nauchnoj Shkoly' Kompressorostroeniya SPbGTU [E'lektronny'j Resurs]: (Sb.ref. st. po Publikaciyam i Rabotam Osnovatelya Nauch. Shk. Prof. K.P.Selezneva i ego Uchenikov).—Zagl. s Titul. e'Krana.E'Lektron. Versiya Pech. Publikacii 2000 g.—Dostup iz Lokal'noj Seti IBK SPbPU (Chtenie).—Tekstovy'j Fajl. Available online: https://elib.spbstu.ru/dl/local/107.pdf (accessed on 27 December 2021).
18. International Organization for Standardization. *ISO 5389:2005. Turbocompressors—Performance Test Code*; International Organization for Standardization: Geneva, Switzerland, 2005.
19. Simon, H.; Bülskämper, A. On the Evaluation of Reynolds Number and Relative Surface Roughness Effects on Centrifugal Compressor Performance Based on Systematic Experimental Investigations. *J. Eng. Gas Turbines Power* **1984**, *106*, 489–498. [CrossRef]
20. Ivanov, V.; Kozhukhov, Y.; Nguyen, M.H. Head Math Model for The Low-Flow Impellers of the Centrifugal Compressors. *E3S Web Conf.* **2019**, *140*, 06008. [CrossRef]